## SUPPLEMENTARY METHODS

### Immunostaining

Salispheres were spin down, washed in PBS, fixed in 70% ETOH, embedded in Histogel (Richard-Allan Scientific) and then processed in paraffin. Tissue and salisphere Paraffin sections (4μm) were deparaffined, rehydrated and antigen retrieved (Vector laboratories). Slides were labeled overnight at 4°C with different primary antibodies: anti-c-Kit (R&D Systems), anti-Sca1 (R&D Systems), anti-CK5 (Covance), anti-CK14 (Abcam), anti-CK8 (Hybridoma Bank), anti-Ki67 (Abcam) anti-amylase (Sigma-Aldrich), anit-AQP5 (Alomone Labs), anti GDNF (Abcam), anti GFRα1 (Sigma), anti-RET (Abcam), anti-NCAM (Millipore), anti-phospho-AKT (Cell Signaling), anti- phospho-ERK (Cell Signaling) and anti-phospho-FAK (BD Bioscience). Slides were then incubated with fluorescent secondary antibody (1:200 dilution; Invitrogen) or peroxidase linked secondary antibody (Vector Laboratories). The slides were then mounted with 4', 6-diamidino-2-phenylindole (DAPI, Vector Laboratories) or clear mount (American Master Tech). Images were acquired using a Leica TCS SP2 confocal microscope or Leica DM6000 B upright microscope (Leica Microsystems Inc.)

### HE and PAS staining / Quantification

Paraffin sections were deparaffined, rehydrated and stained with Hematoxylin and Eosin (HE) or Periodic acid Schiff (PAS, Sigma – Aldrich) following manufacturer's instruction. 10 randomly selected PAS stained images were acquired at 200x magnification using a Leica DM6000 B microscope (Leica Microsystems Inc). The percentage of acinar cell area to total measured area was quantified using Image J.

### RNA purification, Reverse Transcription and Quantitative PCR

Total RNA was extracted from sorted cells using RNeasy Kit (Qiagen). Reverse transcription was performed using random hexamer primers (Applied Biosystems). Quantitative PCR was performed on the cDNA samples using a 7900HT detection system (Applied Biosystems). All PCR reactions were carried

out in triplicate. Quantification of the samples was calculated with the threshold cycle by ΔΔCt method. Experiments were repeated four times on different samples.

**MTT Assay**

MTT assay was performed following manufacturer's instruction (Sigma) on Day 1 and Day 14 salispheres in vitro. Signal was measured at 570nm with spectrophotometer.

**Clonogenic Formation Assay**

SMG-C6 or head and neck cancer cell line SCC22A cells were serum starved overnight, followed by 30 min pre-incubation with 100ng/ml GDNF + 150ng/ml GFR$\alpha$1 (R&D Systems). Cells were then irradiated and appropriate dilutions were seeded to 60-mm plates in triplicates 10-14day. The colonies were fixed with 0.1% crystal violet solution in ethanol with 0.1% acidic acid, dried and clones were counted.

**Reactive Oxygen Species Measurement**

SMG-C6 cells were serum starved overnight, followed by 30min preincubation with 100ng/ml GDNF + 150ng/ml GFR$\alpha$1 (R&D Systems). Cells were then incubated with 10 uM DCFH-DA (dichlorofluorescein) and/or 100uM $H_2O_2$ for 20 min, then irradiated with Mark 1 Cesium irradiator at a dose rate of 240.2 R/min (J.L. Shepherd and Associates). DCF was determined on a Synergy H hybrid reader (BioTek) at excitation 475 nm, emission 525 nm respectively.

**Cell Cycle Analysis**

SMG-C6 cells were preincubated with 100ng/ml GDNF + 150ng/ml GFR$\alpha$1 for 30 min (R&D Systems). Cells were then irradiated and cultured for 24 hours to 48 hours. Cells were trypsinized and fixed in ice cold 70% ethanol overnight. After cold PBS wash, cells were stained with 20ug/ml PI with 0.2mg/ml DNAse-free RNAse A, then analyzed on a BD FACS Aria II (BD Biosciences).

**Western Blot**

SMG-C6 cells were serum starved overnight, followed by 30 min preincubation with 100ng/ml GDNF + 150ng/ml GFRα1 (R&D Systems). Cells were then irradiated and collected at different time point with RIPA buffer. 50ug total protein was resolved by SDS-PAGE and transferred to PVDF membranes. Blots were blocked and probed with phospho-γH2AX (Ser139) (Millipore) and tubulin (Cell Signaling Technology).

**Xenograft study**

Six-week old SCID mice were purchased from the Jackson Laboratory and five mice per group were used. Head and neck cancer cell line SCC22A ($5\times10^6$ cells/injection) were implanted into the flanks of each mouse. When the tumor volume reached approximately 100 $mm^3$, 12 Gy was delivered to the tumor with the rest of the body shielded. 24 hours post radiation, 50 μg/mouse GDNF or PBS was injected intra tumor. Tumor size was measured every 1-2 days. Tumor volume was calculated by the formula (π x length x width x height)/6.

**SUPPLEMENTARY FIGURE LEGEND**

**Supplementary Figure 1.** Flow sorting of SMG for different cell surface markers. **(A)** Representative sorting plot for epithelial markers CD24 and EpCAM. $CD24^+$ cells are also positive for EpCAM. **(B)** Representative sorting plots for epithelial marker CD24 and stem cell marker CD49f. $CD24^+$ cells are also positive for CD49f. **(C)** Quantification of salisphere number to seeding cell number of $Lin^-/CD24^+/c\text{-}Kit^+/CD90.1^+$ population and $Lin^-/CD24^+/c\text{-}Kit^-/CD90.1^-$ population at D14 in vitro; n= 3, T-Test. Data are presented as mean+/- SEM.

**Supplementary Figure 2.** SSCs express high level of stem cell markers, proliferate and differentiate in vitro. **(A)** QPCR results show stem cell markers c-Kit, CK5, CK14 are elevated in SSCs compared to $Lin^-/CD24^+/c\text{-}Kit^-/Sca1^-$ cells.

Differentiation marker AQP5 is expressed at a lower level in SSCs. No difference in the expression of the stromal cell marker Vimentin is noted between the two populations; n = 3, T-test, *p<0.05. **(B)** Immunolabeling of stem cell markers c-Kit with Amylase α, Sca1 and CK14 with differentiation marker AQP5 showed minimal co-localization in D21 cultured salisphere. Scale bar 50μm. **(C)** MTT assay shows active metabolism in SSCs compared to the $Lin^-/CD24^-$ or the $Lin^-/CD24^+/c\text{-}Kit^-/Sca1^-$ cells in D14 salispheres; n = 3, T-test, **p<0.01. Data are presented as mean+/- SEM.

**Supplementary Figure 3.** Flow sort of GFP donor submandibular gland. **(A)** Representative sorting plots for the submandibular glands of GFP donor mice. The $GFP^+$ population was first separated with epithelial marker CD24 and hematopoietic cell lineage marker CD45/31. The $Lin^-/CD24^+$ population was further separated with stem cell markers c-Kit and Sca1. **(B)** Salispheres derived form GFP donor mice were positive for GFP. Scale bar 10μm. **(C)** Quantification of salisphere number to seeding cell number for each cell population on D14 in vitro. T-test, **p<0.01, n= 3. Data are presented as mean+/- SEM.

**Supplementary Figure 4.** SSC transplantation improves the morphology of SMG after irradiation. PAS staining of SMG at 13 weeks after SSC implantation. PAS positive cells are functional acinar cells. There are significantly more viable acini in SSC transplanted SMGs. Scale bar 100μm.

**Supplementary Figure 5.** $GFP^+$ SSCs isolated from primary recipients successfully rescue function of SMGs in secondary recipients. **(A)** Total saliva secretion measured at 4 weeks after irradiation (PRT 4w), and 4, 8 and 12 weeks after injection of 250 GFP+ SSCs derived from the primary recipients into each SMG of secondary recipients (Pin 4w, 8w and 12w). T-test, *p<0.05, compared to PRT 4w. Data are presented as mean +/- SEM. **(B)** Representative flow plot of $GFP^+$ SSCs from SMGs of secondary recipients at week 13 after injection of 250 primary $GFP^+$ SSCs into each recipient gland. $GFP^+$ SSCs from primary

recipients differentiated into $CD24^+$ epithelial and $CD24^{low}$ cells, as well as c-$Kit^+$/$Sca1^+$ SSCs in the secondary recipients. **(C)** PAS staining of 2nd recipients' SMGs at 13 weeks after injection of primary SCCs. PAS positive cells reflect functional acini. Scale bar 100μm. **(D)** DAB staining of GFP in 2nd recipients' SMG. Scale bar 100μm. The right panel is a magnified view of the left panel. Scale bar 50μm. Arrows point to secretory ducts and arrowheads point to acini. **(E)** Immunofluorescent staining of GFP and CK14 (red). Arrowheads point to GFP and CK14 positive cells located at the basal layer of the secretory duct in SMG. Scale bar 50μm. **(F)** Immunofluorescent staining of GFP and Sca1 in a D21 salisphere derived from the SSCs isolated from the 2nd recipients' SMG. Scale bar 50μm.

**Supplementary Figure 6**. GDNF signaling pathway in SMG. **(A)** GDNF and **(B)** GFRα1 were highly expressed in the ductal structures of human SMG. Scale bar 50μm. **(C)** GDNF co-localized with GFRα1 in murine SMG at the ductal structure. Scale bar 10μm. **(D)** RET signal could be found weakly in both ductal and acinar structures in human SMG. Scale bar 50μm. **(E)** GDNF signaling was significantly elevated in irradiated human SMG. Scale bar 50μm. **(F)** c-Kit (arrows) did not overlap with pAKT (arrowheads) in irradiated human SMG. Scale bar 10μm. **(G)** c-Kit (arrows) minimally overlapped with pERK (arrowheads) in irradiated human SMG. Scale bar 10μm.

**Supplementary Figure 7.** Injection of GDNF after irradiation successfully rescues SMG function. **(A)** PAS staining of SMG at 8 weeks after irradiation. PAS positive cells are functional acinar cells. Scale bar 100μm. **(B)** Representative flow plot of SMG cells at 8 weeks after Saline/GDNF injection.

**Supplementary Figure 8.** GDNF did not act as a radio-protector in acinar cell line SMG-C6. **(A)** Clonogenic survival of SMG-C6 cells after 4Gy and 8Gy irradiation. T-test, n=3. **(B)** Reactive oxygen species level with or without

radiation treatment (RT), as measured by carboxyl derivative of fluorescein. $H_2O_2$ served as positive control. T-test, *p<0.05, compared to the PBS control (n = 3). **(C)** DNA double strand break marker phospho-H2AX expression after 4Gy irradiation. **(D)** Irradiation induced G1 arrest in SMG-C6 cells. The cell cycle patter was not different between GDNF and PBS treated controls. Data are presented as mean+/- SEM.

**Supplementary Figure 9.** GDNF did not affect HNC tumor growth or response to irradiation. **(A)** Clonogenic survival of SCC22A head and neck cancer cells after 4 Gy and 8 Gy irradiation. **(B)** SCC22A tumor volume before and after 12 Gy irradiation. GDNF or PBS was injected 24 hours after irradiation. T-test, n= 5 mice per group. Data are presented as mean+/- SEM.

**Supplementary Figure 10.** Submandibular gland Irradiation Procedure. **(A)** Mouse jig with 4 shields **(B)** Anesthetized mice positioned in the center of the jig with the rest of the body covered with shields. **(C)** The IC-225 Specimen Irradiation System with the mouse jig at the calculated distance from the source. **(D)** Anesthetized mice positioned in the center of the jig, aligning with the source.

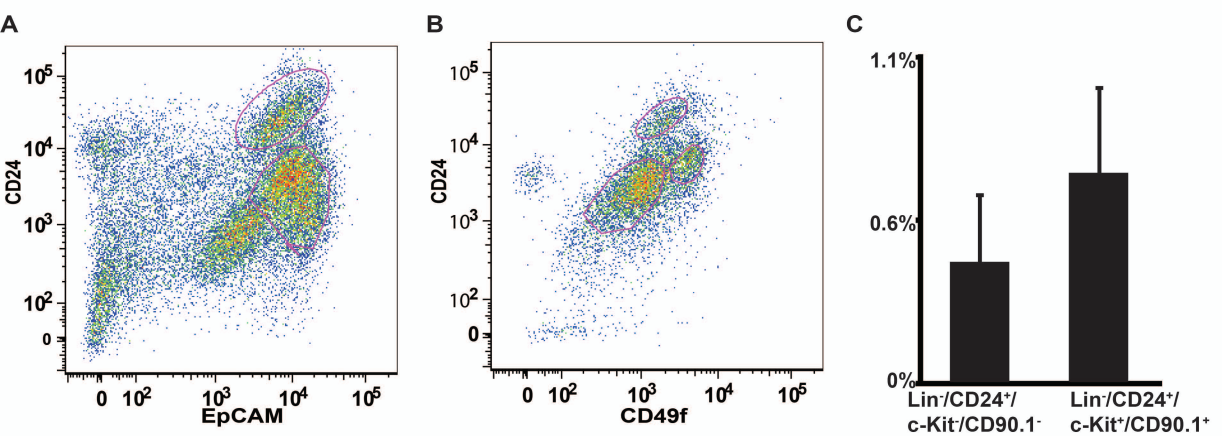


**Supplementary Figure 1.** Flow sorting of SMG for different cell surface markers. **(A)** Representative sorting plot for epithelial markers CD24 and EpCAM. $CD24^+$ cells are also positive for EpCAM. **(B)** Representative sorting plots for epithelial marker CD24 and stem cell marker CD49f. $CD24^+$ cells are also positive for CD49f. **(C)** Quantification of salisphere number to seeding cell number of $Lin^-/CD24^+/c\text{-}Kit^+/CD90.1^+$ population and $Lin^-/CD24^+/c\text{-}Kit^-/CD90.1^-$ population at D14 in vitro; n= 3, T-Test. Data are presented as mean+/- SEM.

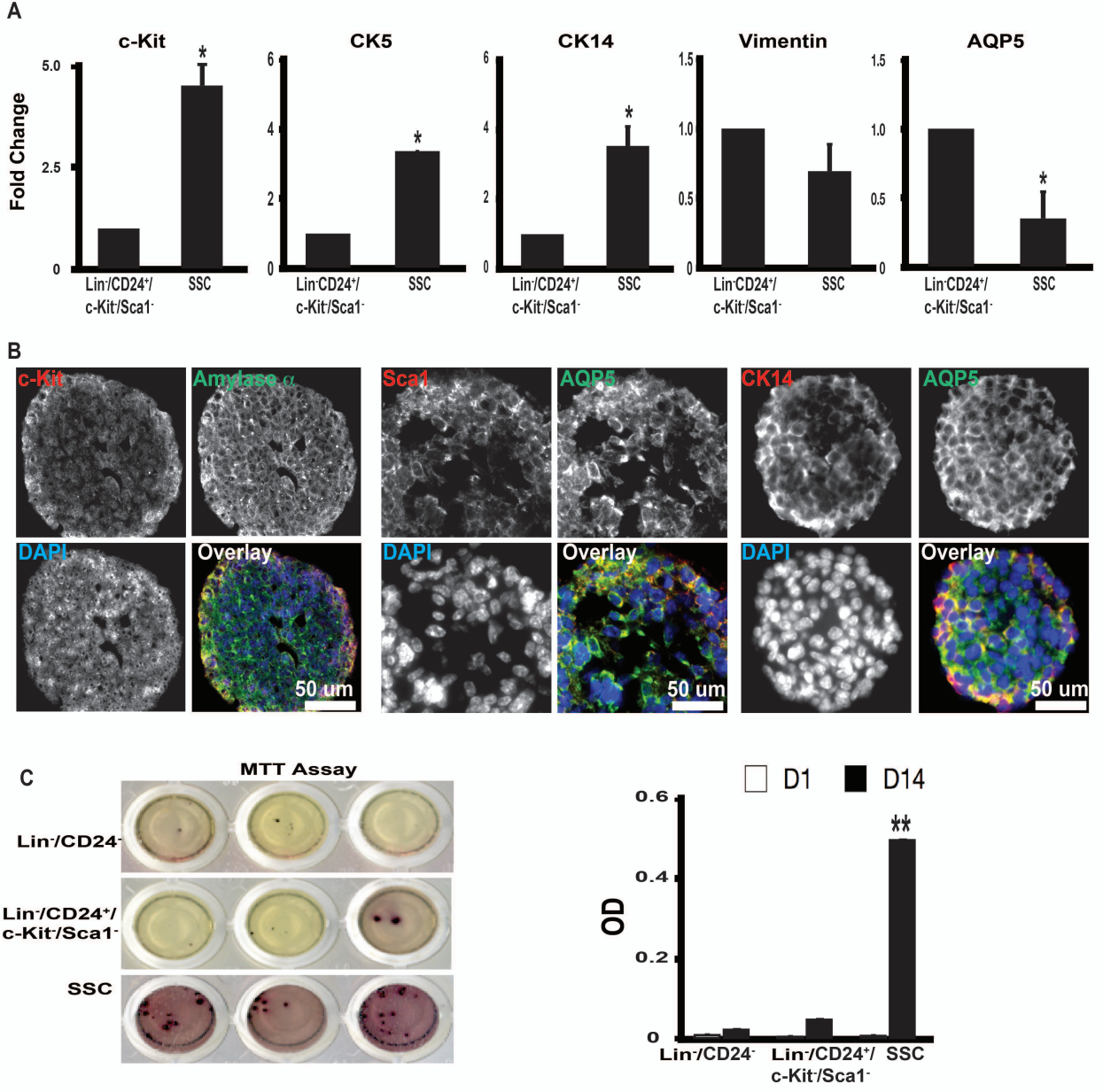


**Supplementary Figure 2.** SSCs express high level of stem cell markers, proliferate and differentiate in vitro. **(A)** QPCR results show stem cell markers c-Kit, CK5, CK14 are elevated in SSCs compared to Lin$^-$/CD24$^+$/c-Kit$^-$/Sca1$^-$ cells. Differentiation marker AQP5 is expressed at a lower level in SSCs. No difference in the expression of the stromal cell marker Vimentin is noted between the two populations; n = 3, T-test, *p<0.05. **(B)** Immunolabeling of stem cell markers c-Kit with Amylase α, Sca1 and CK14 with differentiation marker AQP5 showed minimal co-localization in D21 cultured salisphere. Scale bar 50μm. **(C)** MTT assay showed active metabolism in SSCs compared to the Lin-/CD24- or the Lin$^-$/CD24$^+$/c-Kit$^-$/Sca1$^-$ cells in D14 salispheres; n = 3, T-test, **p<0.01. Data are presented as mean+/- SEM.

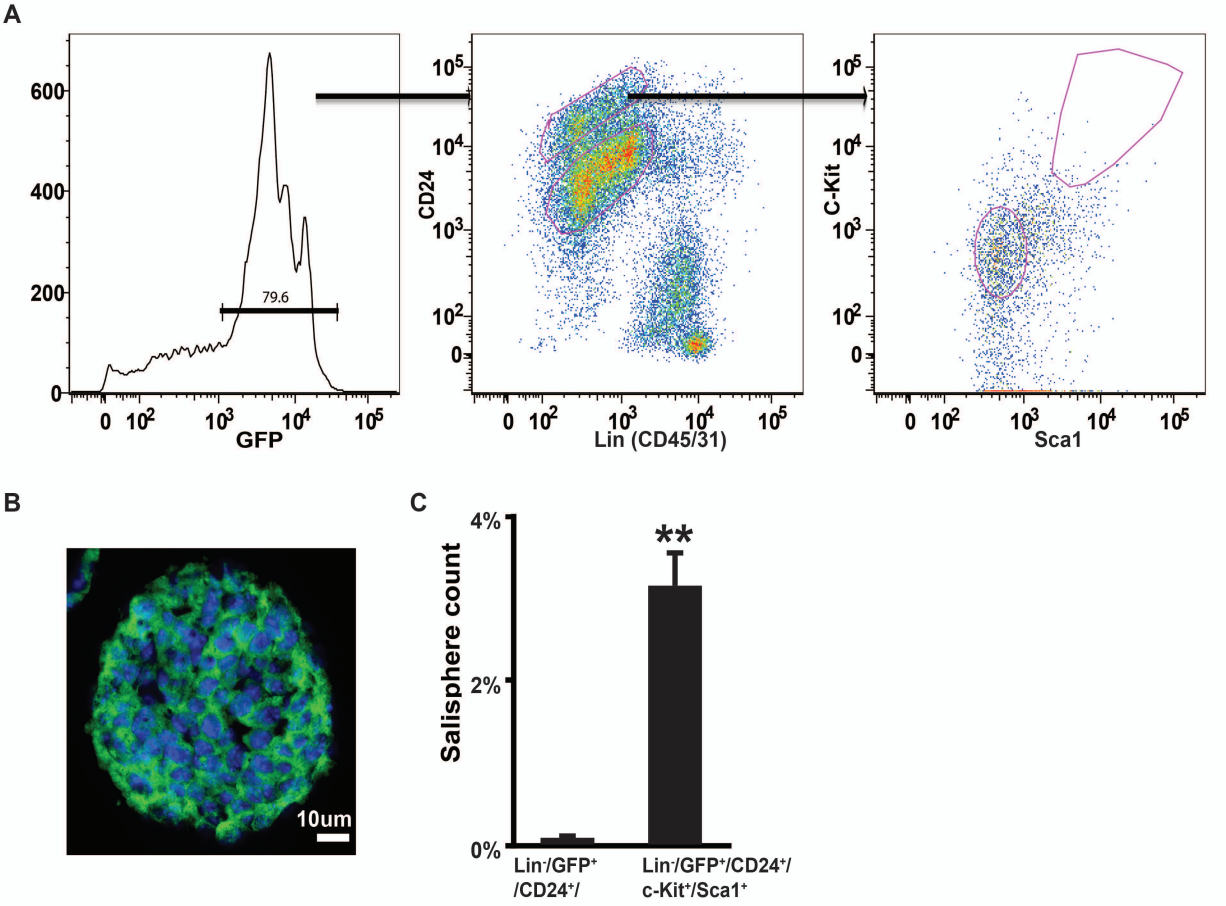


**Supplementary Figure 3.** Flow sort of GFP donor submandibular gland. **(A)** Representative sorting plots for the submandibular glands of GFP donor mice. The $GFP^+$ population was first separated with epithelial marker CD24 and hematopoietic cell lineage marker CD45/31. The $Lin^-/CD24^+$ population was further separated with stem cell markers c-Kit and Sca1. **(B)** Salispheres derived form GFP donor mice were positive for GFP. Scale bar 10μm. **(C)** Quantification of salisphere number to seeding cell number for each cell population on D14 in vitro. T-test, **p<0.01, n= 3. Data are presented as mean+/- SEM.

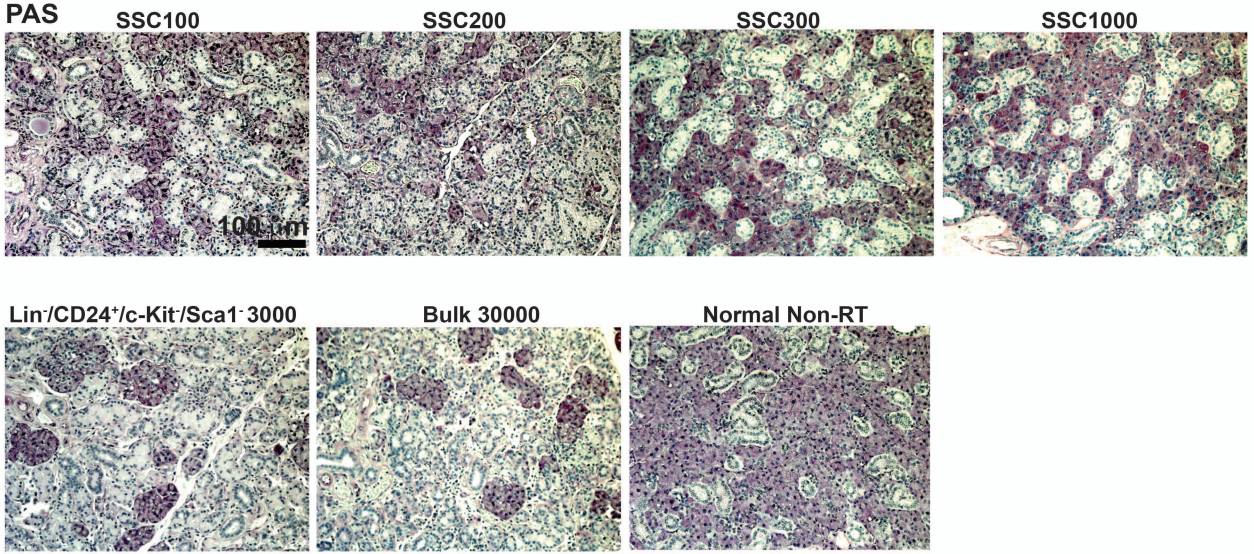


**Supplementary Figure 4.** SSCs transplantation improves the morphology of SMG after irradiation. PAS staining of SMG at 13 weeks after SSC implantation. PAS positive cells are functional acinar cells. There are significantly more viable acini in SSC transplanted SMGs.Scale bar 100μm.

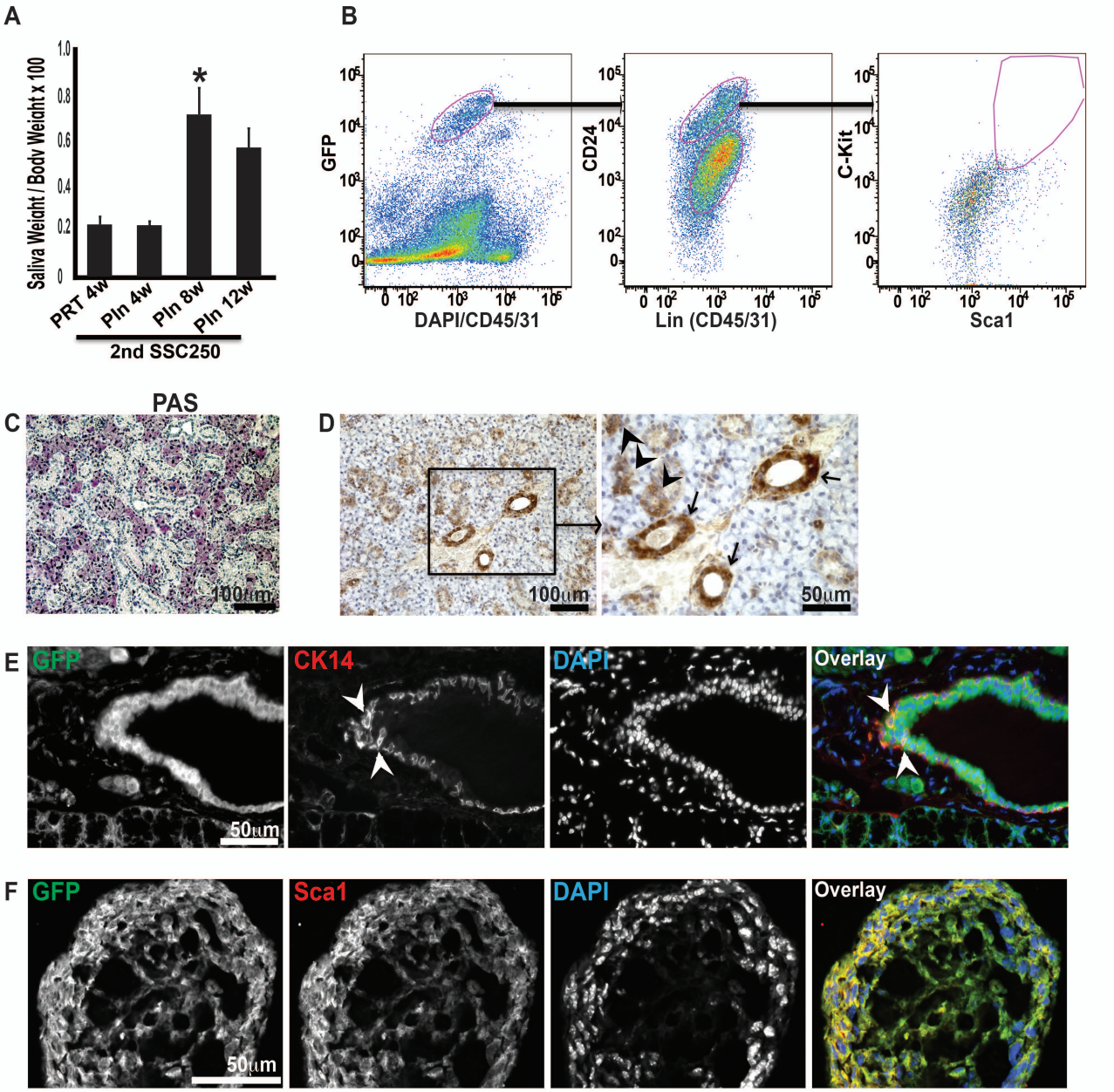


**Supplementary Figure 5.** GFP$^+$ SSCs isolated from primary recipients successfully rescue function of SMGs in secondary recipients. **(A)** Total saliva secretion measured at 4 weeks after irradiation (PRT 4w), and 4, 8 and 12 weeks after injection of 250 GFP$^+$SSCs derived from the primary recipients into each SMG of secondary recipients (Pin 4w, 8w and 12w). T-test, *p<0.05, compared to PRT4w. Data are presented as mean +/- SEM. **(B)** Representative flow plot of GFP$^+$ SSCs from SMGs of secondary recipients at week 13 after injection of 250 primary GFP$^+$ SSCs into each recipient gland. GFP$^+$ SSCs from primary recipients differentiated into CD24$^+$ epithelial and CD24$^{low}$ cells, as well as c-Kit$^+$/Sca1$^+$ SSCs in the secondary recipients. **(C)** PAS staining of 2$^{nd}$ recipients' SMGs at 13 weeks after injection of primary SCCs. PAS positive cells reflect functional acini. Scale bar 100μm. **(D)** DAB staining of GFP in 2$^{nd}$ recipients' SMG. Scale bar 100μm. The right panel is a magnified view of the left panel. Scale bar 50μm. Arrows point to secretory ducts and arrowheads point to acini. **(E)** Immunofluorescent staining of GFP and CK14 (red). Arrowheads point to GFP and CK14 positive cells located at the basal layer of the secretory duct in SMG. Scale bar 50μm.**(F)** Immunofluorescent staining of GFP and Sca1 in a D21 salisphere derived from the SSCs isolated from the 2nd recipients' SMG. Scale bar 50μm.

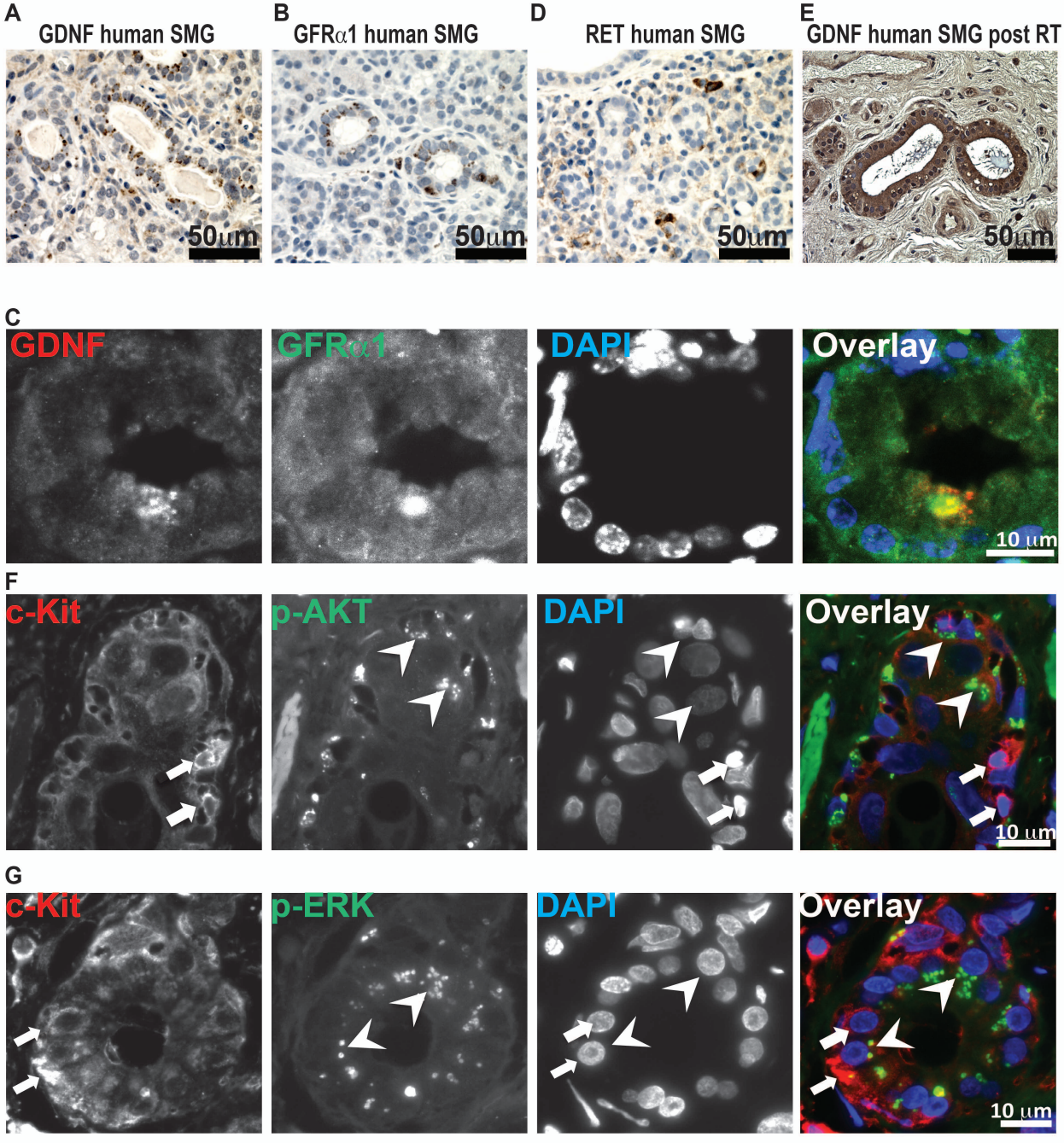


**Supplementary Figure 6.** GDNF signaling pathway in SMG. **(A)** GDNF and **(B)** GFRα1 were highly expressed in the ductal structures of human SMG. Scale bar 50μm. **(C)** GDNF co-localized with GFRα1 in murine SMG at the ductal structure. Scale bar 10μm. **(D)** RET signal could be found weakly in both ductal and acinar structures in human SMG. Scale bar 50μm. **(E)** GDNF signaling wa significantly elevated in irradiated human SMG. Scale bar 50μm. **(F)** c-Kit (arrows) did not overlap with pAKT (arrowheads) in irradiated human SMG. Scale bar 10μm. **(G)** c-Kit (arrows) minimally overlapped with pERK (arrowheads) in irradiated human SMG. Scale bar 10μm.

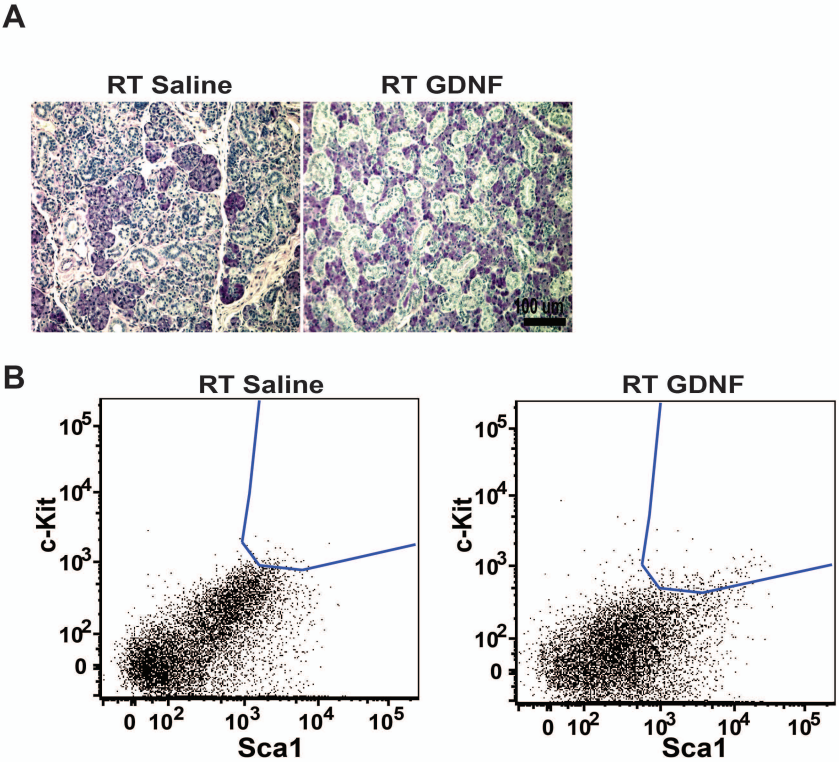


**Supplementary Figure 7.** Injection of GDNF after irradiation successfully rescues SMG function. **(A)** PAS staining of SMG at 8 weeks after irradiation. PAS positive cells are functional acinar cells. Scale bar 100μm. **(B)** Representative flow plot of SMG cells at 8 weeks after Saline/GDNF injection.

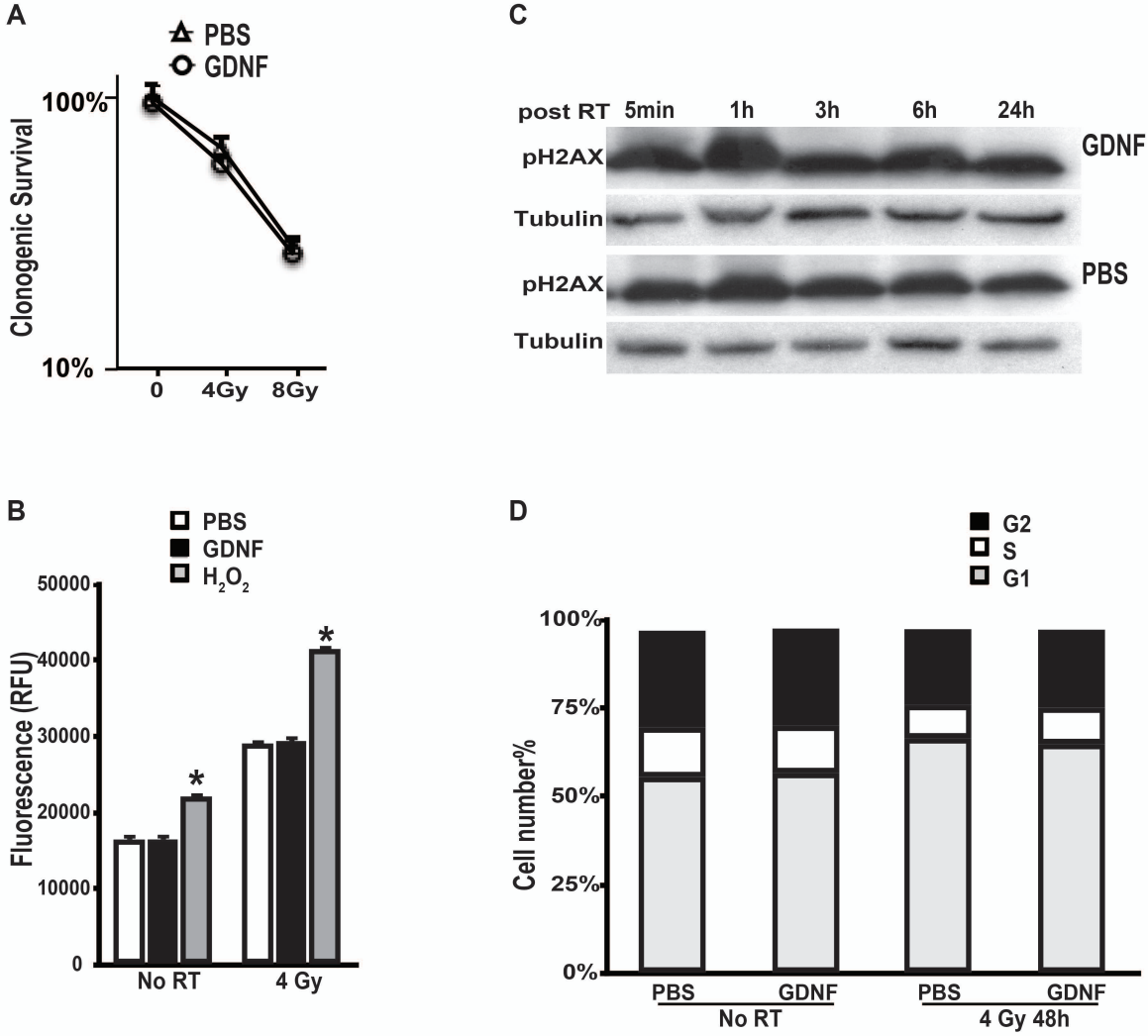


**Supplementary Figure 8.** GDNF did not act as a radio-protector in acinar cell line SMG-C6. **(A)** Clonogenic survival of SMG-C6 cells after 4Gy and 8Gy irradiation. T-test, n=3. **(B)** Reactive oxygen species level with or without radiation treatment (RT), as measured by carboxyl derivative of fluorescein. $H_2O_2$ served as positive control. T-test, *$p<0.05$, compared to the PBS control (n = 3). **(C)** DNA double strand break marker phospho-H2AX expression after 4Gy irradiation. **(D)** Irradiation induced G1 arrest in SMG-C6 cells. The cell cycle pattern was not different between GDNF and PBS treated controls. Data are presented as mean +/- SEM.

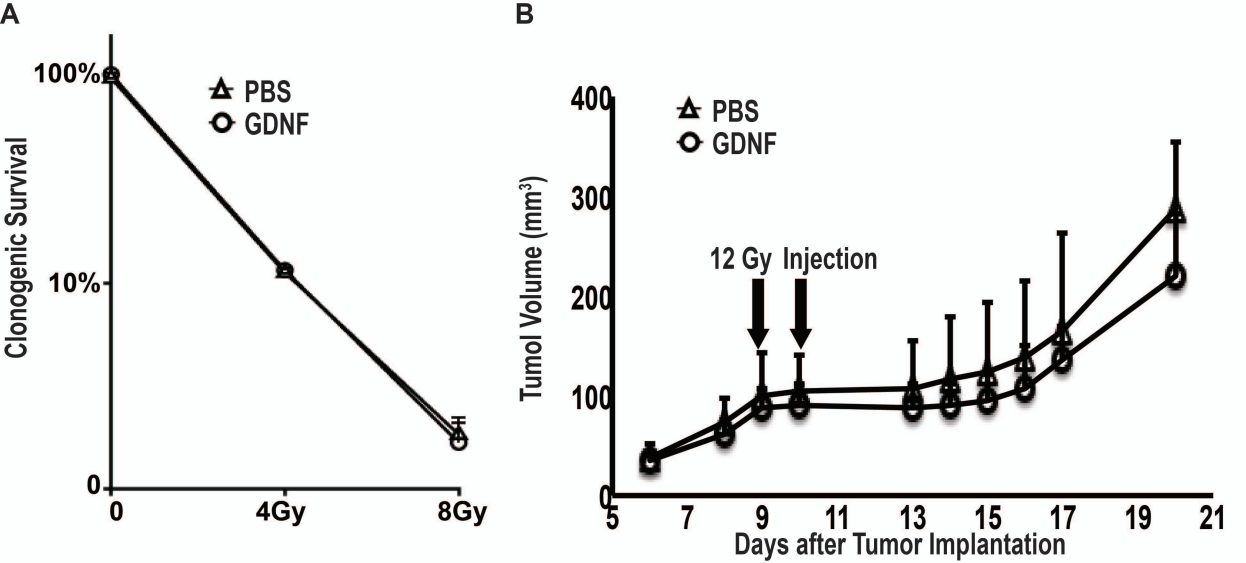


**Supplementary Figure 9.** GDNF did not afffect HNC tumor growth or response to irradiation. **(A)** Clonogenic survival of SCC22A head and neck cancer cells after 4 Gy and 8 Gy irradiation. **(B)** SCC22A tumor volume before and after 12 Gy irradiation. GDNF or PBS was injected 24 hours after irradiation. T-test, n= 5 mice per group. Data are presented as mean +/- SEM.

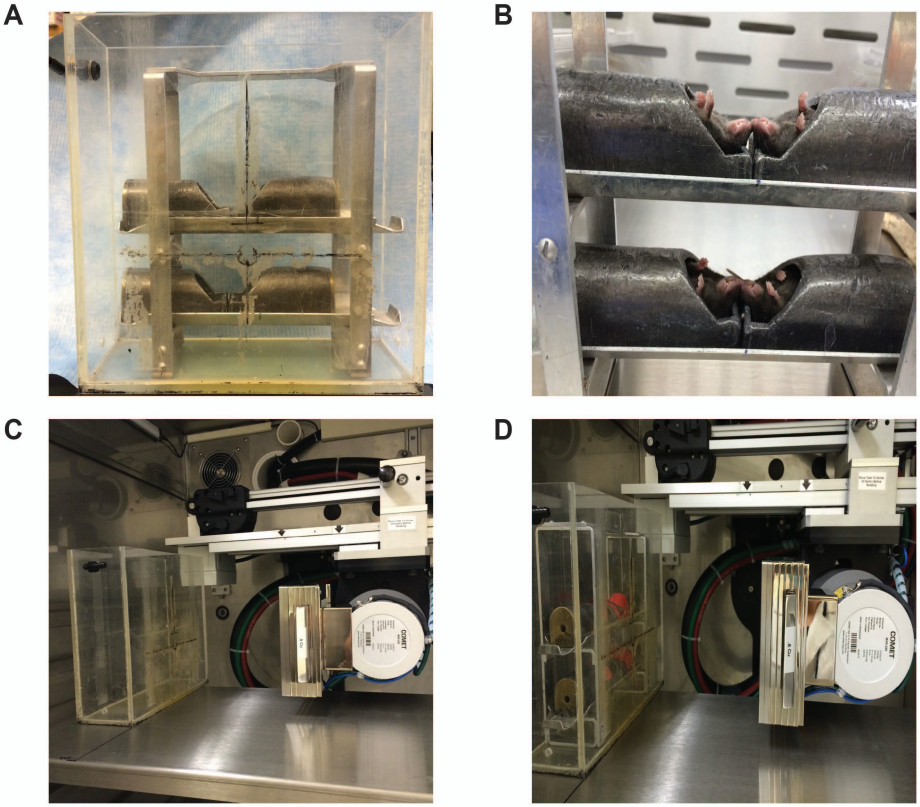


**Supplementary Figure 10.** Submandibular gland Irradiation Procedure. **(A)** Mouse jig with 4 shields **(B)** Anesthetized mice positioned in the center of the jig with the rest of the body covered with shields. **(C)** The IC-225 Specimen Irradiation System with the mouse jig at the calculated distance from the source. **(D)** Anesthetized mice positioned in the center of the jig, aligning with the source.

**Table S1. Strategy and Labeling of SMG Sorting.**

| Population | Description | Sub Population | Description | Sub population: Parent population% |
|---|---|---|---|---|
| P1 | FSC/SSC | | | |
| P2 | FSH/FSW | | | |
| P3 | SSH/SSW | | | |
| P4 | $DAPI^-$ | | | P5:P4 14.8%<br>P6:P4 63.1%<br>P19:P6 33%<br>P20:P6 25% |
| P5 | $Lin^-/CD24^+$ ($CD45/31^-/CD24^+$) | P7 | $c\text{-}kit^{high}/sca1^-$ | P7:P5 0.208% |
| | | P8 | $c\text{-}kit^+/sca1^+$ | P8:P5 0.373% |
| | | P9 | $c\text{-}kit^-/sca1^{high}$ | P9:P5 0.171% |
| | | P10 | $c\text{-}kit^-/sca1^-$ | P10:P5 47.9% |
| | | P13 | $c\text{-}kit^{low}/sca1^-$ | P13:P5 0.208% |
| | | P14 | $c\text{-}kit^-/sca1^{low}$ | P14:P5 6.77% |
| P6 | $Lin^-/CD24^{low}$ & $Lin^-/CD24^-$ | P11 | $c\text{-}kit^{high}/sca1^-$ | P11:P6 5.7% |
| | | P12 | $c\text{-}kit^-/sca1^-$ | P12:P6 32.1% |
| | | P15 | $c\text{-}kit^-/sca1^{low}$ | P15:P6 6.91% |
| P19 | $Lin^-/CD24^{low}$ | P16 | $c\text{-}kit^+/sca1^+$ | P16:P19 0.185% |
| | | P18 | $c\text{-}kit^-/sca1^{high}$ | P18:P19 3.45% |
| P20 | $Lin^-/CD24^-$ | P17 | $c\text{-}kit^-/sca1^{high}$ | P17:P20 1.58% |

**FSC**: forward scatter, **SSC**: side scatter, **FSH**: forward scatter height, **FSW**: forward scatter width, **SSH**: side scatter height, **SSW**: side scatter width. Sorting strategy and labeling of each population; high/ low represents relative expression level.

**Table S2. Functional Annotation Chart Summary**

| Category | Gene Count | Genes | P Value |
|---|---|---|---|
| Signal Pathway | 82 | KLK1B8, KLK1B11, KLK1B3, CACHD1, KLK1B4, KLK1B5, JAG2, CXCL12, **GDNF**, PDCD1, MMRN2, INSRR, CXCL10, WISP1, RSPO1, HTRA1, SOSTDC1, TGFBI, ROBO2, WNT6, VWA2, RAMP3, WNT10A, ICAM1, UCMA, WNT10B, EFNB3, PDPN, KLK1B24, PTPRS, MGP, TMEM132A, ARTN, NRXN1, SLIT2, MOXD1, MMP11, THBD, ADM, F3, PLXDC2, LAMB1-1, ADAMTS1, LAMC2, NGFR, ADAMTS2, SMR3A, TG, FGFR3, ENPP2, DCN, CDH3, TIMP3, ISLR, LY6A, VCAM1, SMOC2, LAMB3, FGG, LY6D, SHISA4, MSLN, BAI2, PTN, SLC39A4, OLFM1, LY6C1, IL18R1, EFEMP1, KLK1, PCDH19, DNASE1, IGSF21, FBLN1, GPR37, FBLN2, CP, ANTXR1, IGFL3, MEGF6, BMP7, IGFBP5 | 6.05E-19 |
| Disulfide Bond | 68 | KLK1B8, KLK1B11, KLK1B3, KLK1B4, KLK1B5, JAG2, CXCL12, **GDNF**, PDCD1, MMRN2, INSRR, CXCL10, WISP1, RSPO1, SOSTDC1, TGFBI, ROBO2, VWA2, RAMP3, ICAM1, EFNB3, MMEL1, KLK1B24, PTPRS, ARTN, MGP, NRXN1, SLIT2, MOXD1, MMP11, THBD, ADM, F3, LAMB1-1, ADAMTS1, LAMC2, NGFR, ADAMTS2, TG, C3AR1, FGFR3, ENPP2, DCN, TIMP3, ISLR, VCAM1, LY6A, SMOC2, LAMB3, FGG, LY6D, BAI2, PTN, OLFM1, LY6C1, IL18R1, LGALS3, EFEMP1, KLK1, DNASE1, IGSF21, FBLN1, GPR37, FBLN2, CP, MEGF6, BMP7, IGFBP5 | 5.57E-15 |

| | | | |
|---|---|---|---|
| Secreted Proteins | 47 | TG, ENPP2, DCN, **GDNF**, CXCL12, TIMP3, CXCL10, MMRN2, ISLR, SMOC2, LAMB3, FGG, WISP1, RSPO1, HTRA1, SOSTDC1, MSLN, TGFBI, PTN, WNT6, VWA2, WNT10A, UCMA, WNT10B, MMEL1, EFEMP1, LGALS7, ARTN, MGP, SLIT2, MMP11, DNASE1, IGSF21, FBLN1, ADM, FBLN2, SERPINB5, LAMB1-1, LAMC2, ADAMTS1, IGFL3, CP, BMP7, MEGF6, ADAMTS2, SMR3A, IGFBP5 | 1.01E-12 |
| Glycoprotein | 78 | KLK1B8, KLK1B11, KLK1B3, CACHD1, KLK1B5, JAG2, **GDNF**, PDCD1, MMRN2, INSRR, WISP1, RSPO1, SOSTDC1, CHST11, ROBO2, WNT6, KCNQ1, VWA2, RAMP3, WNT10A, ICAM1, WNT10B, EFNB3, PDPN, MMEL1, KLK1B24, PTPRS, ARTN, TMEM132A, NRXN1, SLIT2, MOXD1, KCNT1, THBD, CHST7, SERPINB5, F3, PLXDC2, LAMB1-1, ADAMTS1, LAMC2, NGFR, ADAMTS2, EMP1, TG, C3AR1, FGFR3, ENPP2, DCN, CDH3, ISLR, LY6A, VCAM1, SMOC2, LAMB3, FGG, LY6D, MSLN, BAI2, SLC39A4, OLFM1, LY6C1, IL18R1, SLC12A4, EFEMP1, KLK1, PCDH19, CSGALNACT1, DNASE1, IGSF21, GGT6, FBLN1, GPR37, FBLN2, CP, ANTXR1, MEGF6, BMP7 | 7.28E-12 |
| Extracellular Matrix | 17 | WNT10A, WNT10B, UCMA, DCN, TIMP3, MMP11, MMRN2, SMOC2, LAMB3, FBLN1, FBLN2, TGFBI, LAMB1-1, ADAMTS1, LAMC2, WNT6, ADAMTS2 | 5.89E-10 |
| Zymogen | 11 | KLK1B8, GGT6, CASP4, KLK1B11, KLK1B3, KLK1B5, KLK1B24, ADAMTS1, KLK1, ADAMTS2, MMP11 | 3.82E-05 |
| Developmental Protein | 22 | MDFI, WNT10A, WNT10B, EFNB3, TBX2, PDPN, JAG2, MGP, DACH1, SLIT2, UHRF1, PAK3, DDX25, GM11223, ROBO2, STMN1, ID3, NGFR, BMP7, WNT6, GADD45B, SIK1, OLFM1 | 8.77E-05 |
| Calcium Binding | 6 | DNASE1, FBLN1, FBLN2, LAMB1-1, MGP, CDH3 | 1.13E-04 |
| Basement Membrane | 5 | SMOC2, FBLN1, LAMB3, LAMB1-1, LAMC2 | 3.81E-04 |
| Chemotaxis | 6 | C3AR1, ENPP2, ROBO2, CXCL12, SLIT2, CXCL10 | 4.21E-04 |

| | | | |
|---|---|---|---|
| EGF-like Domain | 10 | FBLN1, THBD, FBLN2, FAT2, EFEMP1, JAG2, NRXN1, MEGF6, SLIT2, VWA2 | 4.66E-04 |
| Cell Adhesion | 13 | ICAM1, PTPRS, NRXN1, CDH3, PCDH19, VCAM1, LAMB3, WISP1, PKP1, TGFBI, MSLN, LAMB1-1, LAMC2 | 5.40E-04 |
| Apoptosis | 12 | FAM176A, DAPL1, DNASE1, CASP4, SERPINA3G, CSRNP1, LGALS7, NGFR, TNFAIP3, GADD45B, PDCD1, WDR92 | 6.99E-04 |
| Serine Proteinase | 5 | KLK1B8, KLK1B11, KLK1B3, KLK1B5, KLK1 | 9.45E-04 |
| Wnt Signaling Pathway | 7 | WNT10A, WNT10B, WISP1, RSPO1, SOSTDC1, LEF1, WNT6 | 1.33E-03 |
| Calcium | 18 | CACHD1, EFEMP1, JAG2, NRXN1, CDH3, S100A14, PCDH19, MMP11, SMOC2, DNASE1, FGG, FBLN1, KCNT1, CAMK4, FBLN2, FAT2, CACNA1G, MEGF6 | 1.34E-03 |
| Growth Factor | 7 | KLK1B3, KLK1B4, ARTN, PTN, BMP7, **GDNF**, CXCL12 | 1.93E-03 |
| Differentiation | 13 | MDFI, LGALS3, EFNB3, MGP, SLIT2, DAPL1, DDX25, GM11223, ROBO2, STMN1, NGFR, SIK1, GADD45B, BMP7 | 2.73E-03 |
| Submandibular Gland | 3 | KLK1B3, KLK1B4, KLK1B5 | 2.78E-03 |
| Blocked Carboxyl End | 3 | LY6A, VCAM1, LY6D | 2.78E-03 |
| Protease | 13 | KLK1B8, KLK1B11, KLK1B3, MMEL1, KLK1B5, KLK1B24, KLK1, MMP11, CASP4, HTRA1, ADAMTS1, TNFAIP3, ADAMTS2 | 6.09E-03 |
| Serine protease | 7 | KLK1B8, KLK1B11, KLK1B3, HTRA1, KLK1B5, KLK1B24, KLK1 | 6.76E-03 |
| Phosphatidylinositol linkage | 3 | LY6A, VCAM1, LY6D | 7.49E-03 |

| | | | |
|---|---|---|---|
| Cleavage on pair of Basic Residues | 8 | ADM, ENPP2, MSLN, ADAMTS1, CDH3, **GDNF**, MMP11, INSRR | 1.12E-02 |
| gamma-Carboxyglutamic Acid | 3 | UCMA, TGFBI, MGP | 1.42E-02 |
| Heparin-Binding | 4 | RSPO1, PTN, LAMC2, ADAMTS1 | 1.68E-02 |
| Laminin EGF-like Domain | 3 | LAMB3, LAMB1-1, LAMC2 | 3.50E-02 |
| GPI-Anchor | 5 | LY6A, LY6C1, VCAM1, LY6D, MSLN | 3.82E-02 |
| Intermediate Filament | 4 | KRT5, KRT17, KRT15, KRT14 | 3.99E-02 |
| Sulfation | 3 | TG, C3AR1, UCMA | 4.69E-02 |